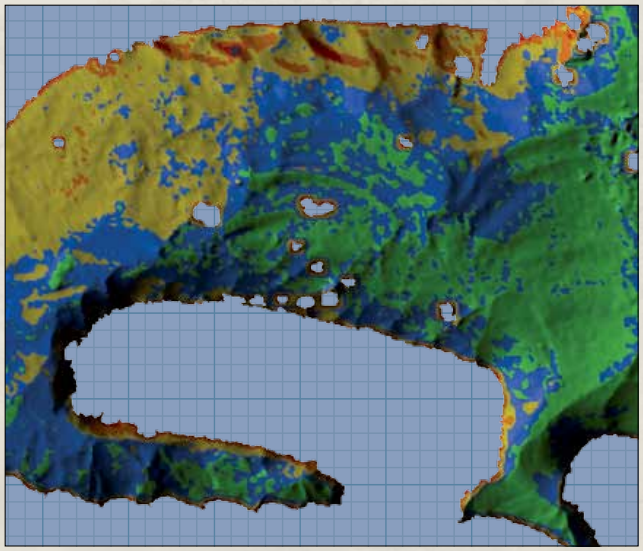

Appendix B

3D Scanning of the Eccentric Cherts and Bifaces from the Rosalila Cache

Alexandre Tokovinine
Peabody Museum of Archaeology and Ethnology, Harvard University

The on-going project of 3D documentation of Copan sculptures by the Corpus of Maya Hieroglyphic Inscriptions of the Peabody Museum of Archaeology and Ethnology created additional opportunities to explore the application of the technology to a wider set of artifacts and materials. One of these sideline projects centered on chert artifacts known as "eccentrics" or often referred to as "eccentric flints."

The principal goal of 3D scanning of the nine eccentric cherts and three bifaces from the Rosalila cache was to facilitate measurement and study of these elaborate stone artifacts without endangering fragile textile fragments adhering to their surface. The digital record would assist in the conservation of the textiles by potentially reducing the necessity to physically interact with the original artifacts. It would also enable the production of physical replicas.

A structured light system SmartSCAN Duo was used for the documentation. It operates by projecting a pattern of stripes onto the surface captured by two cameras. The cameras and the structured light projector are mounted on the same carbon fiber rod and pre-calibrated. No physical contact with the scanned object is required and the light source is a simple halogen bulb, so the digitizing process is relatively non-invasive. SmartSCAN remains one of the top optical 3D scanners in terms of its XY resolution, precision, flexibility, and accuracy. Each scan generates a point cloud that reflects the surface topography of the object within the scanner's field of view and measurement depth. Multiple digital meshes from point clouds are then aligned and merged into a single 3D model. SmartSCAN is available with different lenses for its projector and cameras which offer progressively higher resolution, precision, and accuracy, but with the tradeoff of an ever smaller field of view and measurement depth. Like any other structured light system, SmartSCAN struggles with capturing high-contrast, translucent, and highly reflective surfaces.

The extremely fragile nature of the textile remains on the eccentric flints meant that scanning had to be done as quickly as possible with minimal exposure to different temperature and moisture and with as little movement of the objects as possible. After some consideration, a specific protocol was established. The artifacts were taken from the vault to the 3D project office which was only several meters away. The artifacts were placed on blocks of Styrofoam on a turntable (Figure B.1a). Turntable and scanner tripod adjustments were sufficient to capture the top textile-covered surface of the artifacts (Figure B.2b). 3D scanning of the other side involved placing the objects on higher Styrofoam supports with a gap in the middle or at the tips of the artifact and positioning the scanner at a slightly oblique angle below (Figure B.3c and d). That avoided the problems that

Facing page: details of Figures B.3 and B.6.

would have been created by flipping the artifacts.

The issue of time was crucial in determining the appropriate field of view and resolution. One option was the field of view with a diagonal of 300 mm. Each scan would be approximately 200x250 mm with a depth of 100 mm (Figure B.2a). The field of view with a diagonal of 90 mm, on the other hand, would cover only 50x75 mm with each capture (Figure B.2b). That said, the larger field of view would produce 3D models with a resolution around 0.2 mm, barely

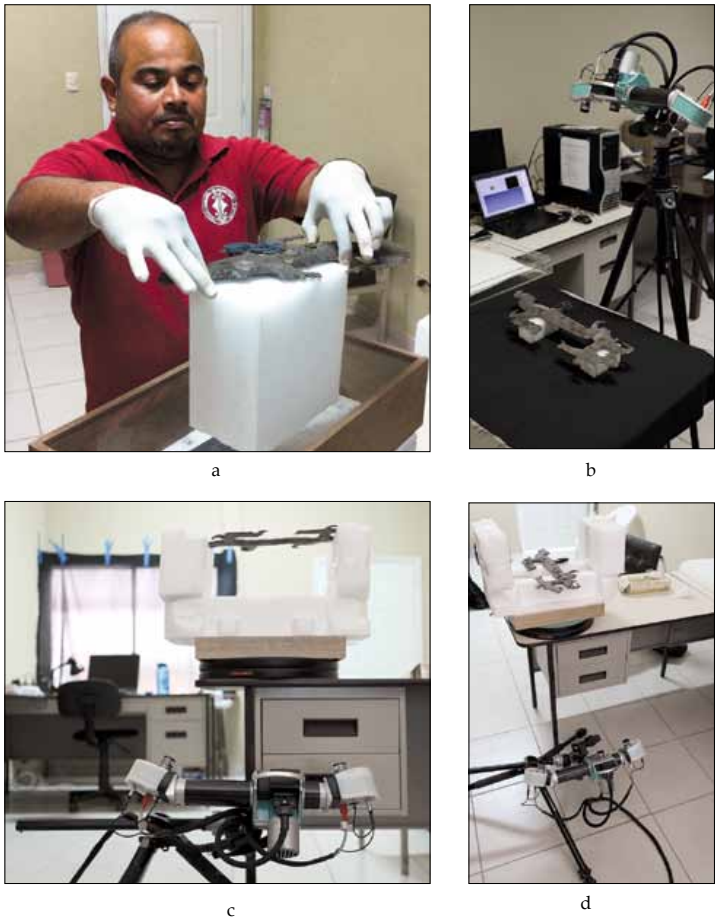

a b c d

Figure B.1. Scanning procedure: (a) museum curator placing the artifact on a Styrofoam support; (b) scanning the top side of the artifact; (c) scanning the middle section of the bottom side; (d) scanning the tip of the bottom side.

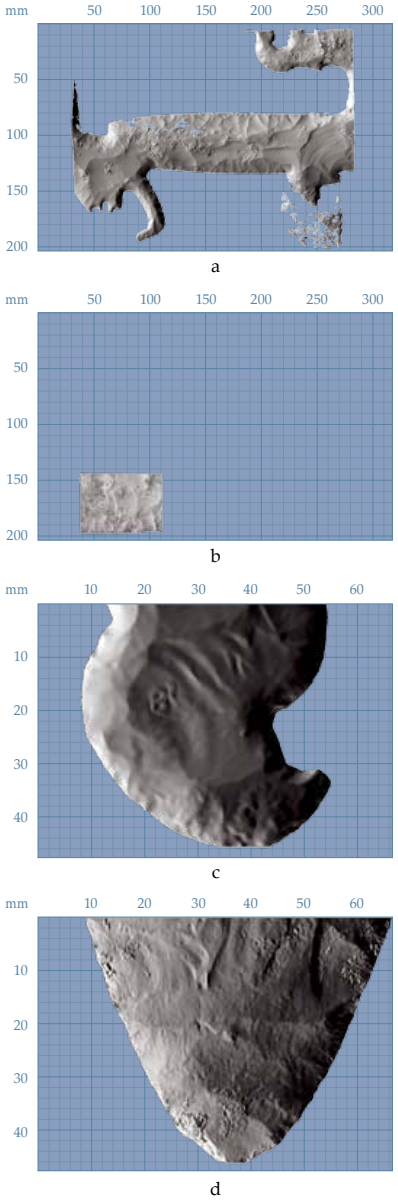

enough to capture key surface details (Figure B.2c). The lens setup with a smaller field of view would lead to much more detailed scans with as little as 0.06 mm between the measurement points (Figure B.2d).

The complex topography of the artifacts, particularly along the edges, meant that multiple shots were required to capture the objects in order to achieve an optimal angle range of 60–88 degrees between every detail of the scanned surface and the scanner. Even with the advantage of a larger field of view and a greater measurement depth, each artifact would require a hundred scans or about five hours of scanning. Consequently, capturing the artifacts at the 90 mm field of view lenses seemed unfeasible. One of the bifaces was documented at that resolution for reference purposes and in order to have a more detailed 3D record of at least some of the textile fragments. A test model of a more complex eccentric was created from the 300 mm field of view data set and examined by the researchers. The quality was deemed adequate for the primary purpose of measurement

Figure B.2. Comparing field of view (FOV) and resolution: (a) a single scan with 300 mm FOV; (b) a single scan with 90 mm FOV; (c) close-up of a 3D model from 300 mm FOV scans; (d) close-up of a 3D model from 90 mm FOV scans (CPN-P-2707/Artifact 90-12 and CPN-P-2758/Artifact 90-1).

and illustration. It was decided, therefore, to scan the other artifacts using the 300 mm field of view lenses.

The surface of the artifacts presented certain challenges for the scanner. Some areas were slightly translucent or had high contrast (very light and very dark spots next to each other). Some textile fragments were reflective because of the protective coating used in conservation. The other sides of the eccentrics were

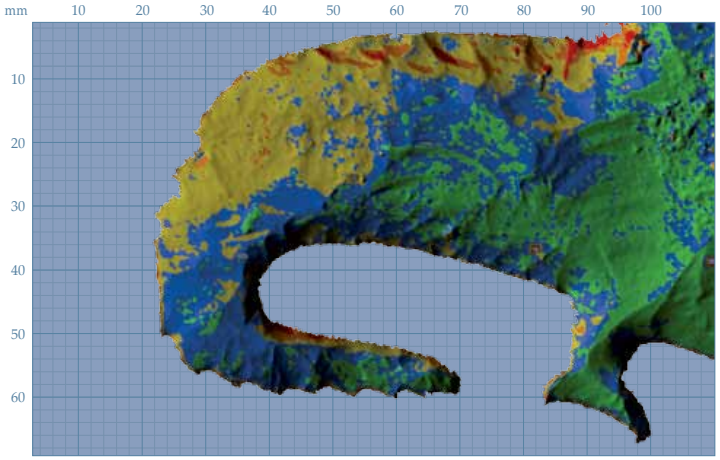

a

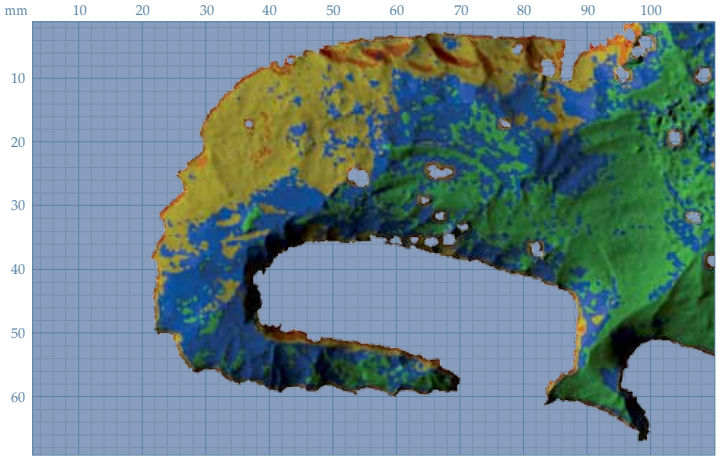

b

Figure B.3. Masking and its effects: (a) single scan with less masking; (b) single scan with more aggressive masking (CPN-P-2707 / Artifact 90-12).

more polished and reflective. Some of these challenges were overcome by using an average of eight captures for each scan and by scanning at a more oblique angle to reduce glare from the projector. Nevertheless, parts of individual scans contained substantial errors and had to be removed manually during processing. It was important to have enough overlap between the scans so that removal of bad sections would not cause gaps in the final model.

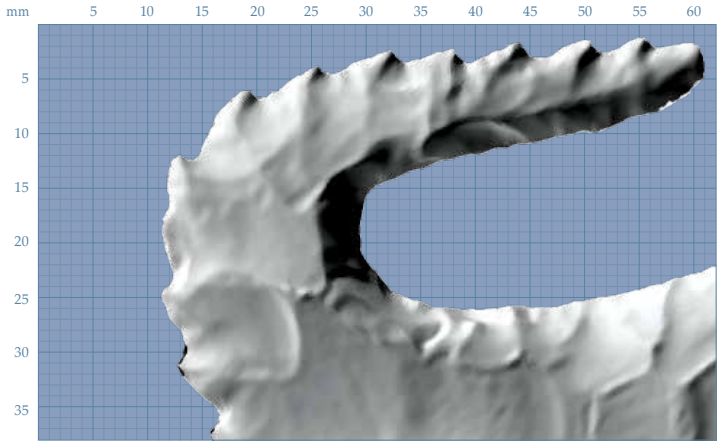

a

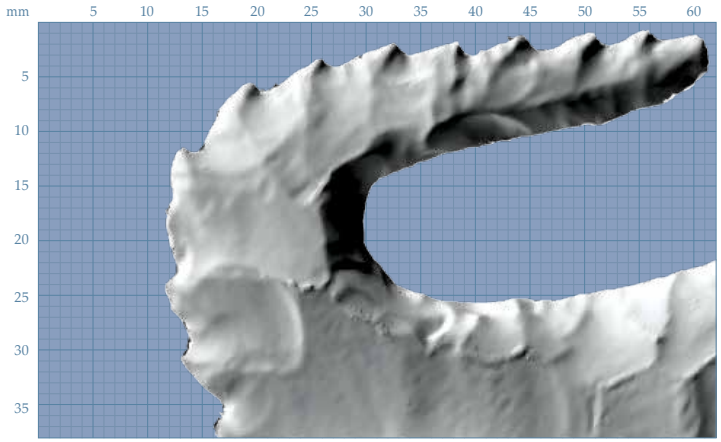

b

Figure B.4. Reliability threshold during scan merger: (a) close-up of a 3D model with high reliability threshold; (b) close-up of a 3D model with low reliability threshold (CPN-P-2707 / Artifact 90-12).

The processing of the data involved additional choices which were made with the goals of the project in mind. The first such choice was the extent to which the pixels along the edges of each scan and in the areas of high contrast had to be masked away. Less masking would result in a 3D surface with more data but potentially more errors (Figure B.3a). Aggressive masking would remove some errors but also simplify the overall surface, particularly at the edges of the scans (Figure B.3b), which would nearly always correspond to the edges of the blades unless they faced the scanner so that both sides of the blade were visible during capture.

The parameters of merging the scans into a single mesh also affected the

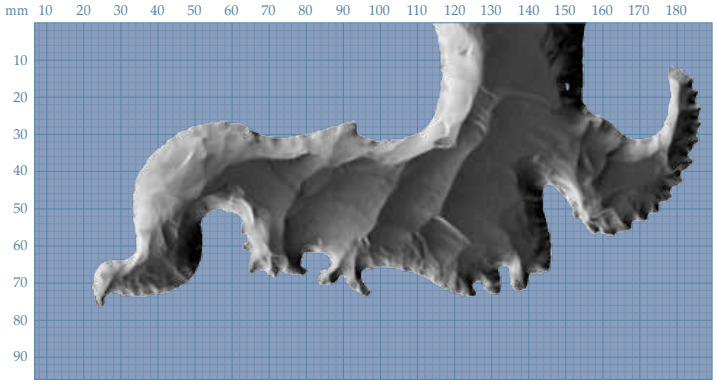

a

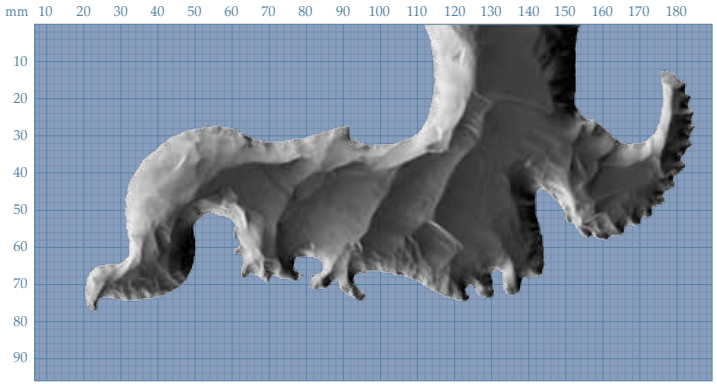

b

Figure B.5. Filling the holes in the mesh: (a) close-up of a 3D model edge with unfilled holes (visible as lighter or darker areas depending on the orientation of surface triangles); (b) close up of a 3D model with filled holes with some edge modification visible (CPN-P-2707/ Art. 90-12).

appearance and potential accuracy of the final 3D model. A greater preference for data taken within a reliable range of angles between the scanner and the artifact would eliminate some surface and edge errors, but would also remove some potentially useful data (Figure B.4a). Introducing less reliable data into the merging process would produce a visibly less regular surface with more detail and more errors (Figure B.4b). Finally, leaving the gaps in the final mesh would make the files unsuitable for 3D printing (Figure B.5a). However, attempts to fill the holes, particularly at the edges, would potentially change the geometry of the edges by cutting some triangles and introducing new ones to fit the shape of the gaps (Figure B.5b). Consequently, it was decided to strive for more data in the merge settings (depending on the overall composition of the data set) and to leave the gaps along the edges unfilled. The resultant 3D models were better suited for measurements and study and less for artistic rendering and physical replication. It is important to emphasize here that the raw scan data remained unchanged, so it may be used again to generate new models with different parameters, for example, with 3D printing in mind.

The finished 3D models were saved as PLY (Stanford Triangle Format) files with color information included. The scanner's own Optocat software was used to make two-dimensional renderings of the models from several view angles with a simulation of multiple raking light sources. Larger images were obtained with free Meshlab software which offered additional filters to enhance the visibility of the surface topography such as radiance scaling (Figure B.6). All renderings were geometrically uniform and distortion-free orthographic views, which could be used for taking measurements and making accurate drawings of the artifacts. Meshlab was also used to downsample the digital models using quadric edge collapse decimation and convert them into U3D (Universal 3D) files, which could be embedded in 3D PDF documents.

Figure B.6. Meshlab-generated grayscale rendering of a 3D model with the radiance scaling filter to enhance the visibility of the surface topography (CPN-P-2707/Artifact 90-12).

Photo: Payson Sheets.

Photo: Ricardo Agurcia F..

References

Agurcia Fasquelle, Ricardo

1996 Rosalila, el corazón de la Acrópolis, El templo del Rey-Sol. *Yaxkin* 14:5-18. Instituto Hondureño de Antropología e Historia, Tegucigalpa.

1997 Le temple du roi Soleil et son évolution au coeur de l'acropole de Copán. In *Les Mayas au Pays de Copán*, pp. 91-100. Skira Editore, Italy.

1998 Copán: Art, Science and Dynasty. In *Maya*, edited by Peter Schmidt, Mercedes de la Garza, and Enrique Nalda, pp. 336-355. Rizzoli, New York.

2004 Rosalila, Temple of the Sun King. In *Understanding Early Classic Copán*, edited by Ellen Bell, Marcello Canuto, and Robert Sharer, pp. 101-112. University of Pennsylvania Museum of Archaeology and Anthropology, Philadelphia.

2007 *Copán: Kingdom of the Sun*. Editorial Transamerica, Tegucigalpa.

Agurcia Fasquelle, Ricardo, and Barbara W. Fash

2005 The Evolution of Structure 10L-16, Heart of the Copán Acropolis. In *Copán: The History of an Ancient Maya Kingdom*, edited by E. Wyllys Andrews and William L. Fash, pp. 201-237. School of American Research Press, Santa Fe.

Agurcia Fasquelle, Ricardo, and William L. Fash, Jr.

1989 Copán: A Royal Maya Tomb Discovered. *National Geographic Magazine* 176(4):481-487.

1991 Maya Artistry Unearthed. *National Geographic Magazine* 180(3):94-105.

Agurcia Fasquelle, Ricardo, and Molly Fierer-Donaldson

2010 Proyecto Oropendola Field Report 2008-2009. Report on file, Instituto Hondureño de Antropología e Historia, Copan.

Agurcia F., Ricardo, Donna K. Stone, and Jorge Ramos

1996 Tierra, tiestos, piedras, estratigrafía y escultura. Investigaciones en la Estructura 10L-16 de Copán. In *Visión del Pasado Maya*, edited by William L. Fash and Ricardo Agurcia F., pp. 185-201. Asociación Copán, Copan.